SCIENTIFIC REPORTS

OPEN

SUBJECT AREAS:
MEMBRANE BIOPHYSICS
ENDOCYTOSIS
MOLECULAR NEUROSCIENCE
NANOSCALE BIOPHYSICS

Received
31 January 2013

Accepted
14 March 2013

Published
28 March 2013

Correspondence and requests for materials should be addressed to P.M.B. (bendix@nbi.dk)

FBAR Syndapin 1 recognizes and stabilizes highly curved tubular membranes in a concentration dependent manner

Pradeep Ramesh[1], Younes F. Baroji[1,2], S. Nader S. Reihani[1,3], Dimitrios Stamou[4,5], Lene B. Oddershede[1,5] & Poul Martin Bendix[1]

[1]Niels Bohr Institute, University of Copenhagen, Blegdamsvej 17, 2100 Copenhagen, Denmark, [2]Department of Physics, Institute for Advanced Studies in Basic Sciences (IASBS), Zanjan 45137-66731, Iran, [3]Department of Physics, Sharif University of Technology, PO BOX 11365-9161 Tehran, Iran, [4]Bionanotechnology and Nanomedicine Laboratory, Department of Chemistry, Nano-Science Center, University of Copenhagen, Universitetsparken 5, 2100 Copenhagen, Denmark, [5]Lundbeck Foundation Center of Excellence for Biomembranes in Nanomedicine.

Syndapin 1 FBAR, a member of the Bin-amphiphysin-Rvs (BAR) domain protein family, is known to induce membrane curvature and is an essential component in biological processes like endocytosis and formation and growth of neurites. We quantify the curvature sensing of FBAR on reconstituted porcine brain lipid vesicles and show that it senses membrane curvature at low density whereas it induces and reinforces tube stiffness at higher density. FBAR strongly up-concentrates on the high curvature tubes pulled out of Giant Unilamellar lipid Vesicles (GUVs), this sorting behavior is strongly amplified at low protein densities. Interestingly, FBAR from syndapin 1 has a large affinity for tubular membranes with curvatures larger than its own intrinsic concave curvature. Finally, we studied the effect of FBAR on membrane relaxation kinetics with high temporal resolution and found that the protein increases relaxation time of the tube holding force in a density-dependent fashion.

Proteins containing BAR domains that can either sense or generate curvature on phospholipid membranes are associated with cellular sites where severe bending of membranes takes place. Working in tandem with a panoply of other host proteins, BAR domain proteins appear to play a crucial role in cellular cargo trafficking through coordinated membrane and cytoskeletal remodeling[1–3]. Consequently, they influence a vast array of physiological activities ranging from T-tubule formation in muscle cells to neuromorphogenesis[1]. In addition, their malfunction is implicated in diseases such as bladder carcinoma, Alzheimer's, and Huntington's, as well as cancer progression[4].

Bar domains belonging to a variety of proteins have been shown to detect membrane morphologies that have a tubular or spherical shape[5–13]. In an experimental assay where a membrane tube is pulled out of a GUV the membrane bound proteins are allowed to freely diffuse between the low curvature compartment (the GUV) and the highly-curved tube, thus mimicking the curvature landscape and connected membrane structures displayed in cells. Proteins containing NBAR domains were shown to up-concentrate on tubular membranes with curvatures that strongly correlated with the BAR domain's high intrinsic curvature[9,11,13,14]. Besides having a concave side, with cationic residues that bind to negatively charged membranes, NBAR domains are also equipped with N-terminal hydrophobic helices which insert into membranes upon binding. These N-terminal helices are implicated in membrane deformation[2] and were found to sense membrane curvature in liposomal assays[7].

FBAR domains, however, are less curved than NBAR domains, and a variety of proteins containing FBAR domains are commonly associated with a range of biological processes where membrane remodeling takes place[1,3,15,16]. The molecular domain curvature differs among the various known species of FBARs with differences in both the degree and the dimensionality of the curvature[3]. In addition, electron micrographs of FBAR domains highlight their ability to self-arrange in an assortment of lattice configurations[17], thus enabling them to aggregate on membranes whose curvatures are higher than the concave curvature of the FBAR domain itself[16]. Interestingly, the FBAR domain of syndapin 1 has a distinctly unique shape when compared to other types of bar domains.

Besides having a shallow curvature on its concave side, the tips of the FBAR domain also point away from the central (long) axis of the protein, giving it a characteristic tilde-shape[16]. Due to this pronounced two dimensional curvature, syndapin 1 can constrict membranes into tubules having a range of curvatures[16] thus giving it an important role in a host of biological functions. Unlike NBAR, syndapin 1 contains two wedge loops that can insert into the hydrophobic region of the bilayer which seem to be critical for its tube forming ability[18].

Sensing of membrane curvatures by the FCHo2 FBAR domain was reported in both a single liposome assay and in a bulk assay with conflicting results[7,19]. The shallow molecular curvature of the FBAR domain's concave side does not necessarily dictate its sensing behavior, since it could bind at an oblique angle to the tube axis[16], or binding could be dominated by membrane insertions of hydrophobic residues displayed on the concave side of the BAR domain[5,7].

To quantify syndapin's curvature sensing behavior, we pulled a membrane nanotube, with controlled diameter, out of a GUV using an optical trap while simultaneously imaging the protein density on the tube and the GUV by confocal fluorescence microscopy. Interestingly, we found an increased sensing of membrane curvature even when the membrane curvature exceeded the protein's intrinsic curvature. By performing force spectroscopy using a photodiode detection system with high temporal resolution of 45 μs, we measured the relaxation behavior of the tube holding force in response to a rapid elongation of the tube. We demonstrate that binding of syndapin affects the relaxation behavior of the pulled tube after rapid elongation, hence, the BAR domains have a mechanical effect on the tube, even at relatively low FBAR concentrations. This conclusion was supported by conducting fluctuation analysis of the thermal motion of free membrane tubes showing that tubes formed in presence of FBAR domains were thinner but still stiffer than spontaneously formed membrane tubes without proteins bound.

Results

Curvature assay. We used an SH3 mutant FBAR domain of syndapin 1 which efficiently binds and deforms membranes but is not autoinhibited by the SH3 domain[20]. The curvature preference of the protein was investigated using membrane nanotubes of variable radii that were pulled out of GUVs held by a suction pipette (see Fig. 1a). The suction pressure was used to regulate the membrane tension thus controlling tube radius[21]. By measuring the tube/GUV intensity ratio versus aspiration pressure we obtained a calibration curve (see Fig. S1 and eq. S1–S2). This ratio was then used in all subsequent measurements to deduce the tube radius from the tube/GUV intensity ratio using a curvature insensitive membrane dye.

The length of the aspirated membrane tongue inside the pipette is proportional to the applied suction pressure and the GUV acts as a reservoir of lipids and proteins. We performed experiments with both artificial lipid mixtures (DOPC:DOPG 3:1) as well as with GUVs made from porcine brain lipid extracts. Fig. 1b shows an overlay of the membrane (red) and protein (white) channels and illustrates syndapin's strong preference for high curvatures (small tube radii) on tubes made from brain lipid extracts. To illustrate the relative tube/GUV intensities of the membrane and protein channel, the intensities of the two respective channels are plotted in Fig. 1c,d as surface plots. The membrane signal of the tube is slightly above background (Fig. 1d), as opposed to the tube's protein signal, which is equivalent to that on the GUV (Fig. 1c), thus showing that the protein has a strong preference for the tube.

Upon gentle aspiration of GUVs decorated with FBAR, membrane tethers were pulled by translating the GUV and micropipette away from the optically trapped particle using a piezo-electric stage controller. The pulling force and the suction system were allowed to briefly equilibrate before initiating confocal acquisition of the membrane and protein channels. Aspiration pressure was then slowly varied, thus effecting a change in tube diameter according to the well-known Laplace relation (see supplementary information, eq. S1–S2). In this manner, we were able to explore a physiologically relevant range of tube diameters, and explicitly quantify protein sorting between the tube and the GUV reservoir as a function of tube diameter and bound density.

Syndapin 1 senses curvature on artificial and brain lipid GUVs. To quantitatively evaluate the sensing characteristics of the FBAR of syndapin 1 we measured the relative density of FBAR on tubes of a range of radii as a function of bulk protein concentration. The protein density on tubes is measured relative to the density on the GUVs and is expressed as a *Sorting* number, according to eq. 1, where *Sorting* = 2 means that the density is two-fold higher on the tube than on the GUV. Sorting is defined as

$$Sorting = \frac{1}{PCF}\frac{(I_{protein}/I_{membrane})_{tube}}{(I_{protein}/I_{membrane})_{GUV}}, \qquad (1)$$

where *PCF* is a polarization dependent correction factor which arises due to the polarization dependence of the membrane incorporated fluorophore[22]. The bound protein density is itself contingent on a host of factors, namely bulk salt and protein concentration, as well as

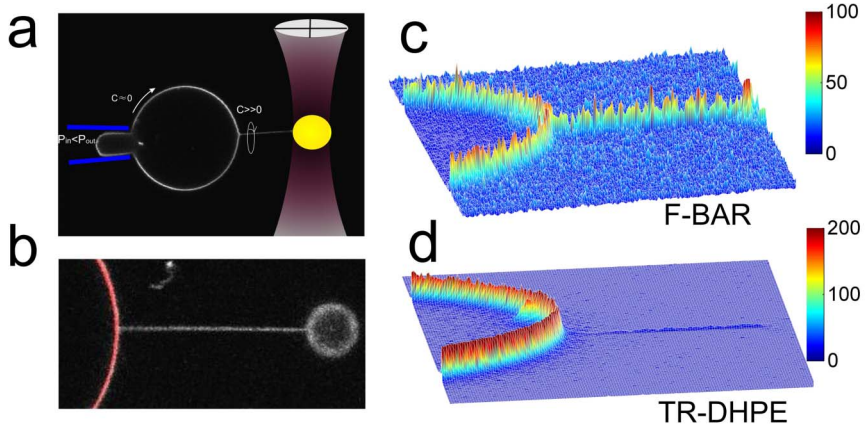

Figure 1 | Assay for testing the curvature preference of syndapin 1. (a) A high curvature brain lipid tube is extracted from a Giant Unilamellar Vesicle (GUV) using optical tweezers. The figure is a composite of a raw data image of the GUV and drawings of the pipette, optical tweezers and the photodiode detection system. (b) Fluorescence intensity is collected from two channels: the membrane channel (red) and the fluorescent FBAR channel (white). The image is an overlay of these two channels showing a significant up-concentration of FBAR on the highly curved tube. (c) and (d) show intensity plots of the FBAR and the TR-DHPE membrane dye, respectively, for a segment of the GUV and the tube.

membrane composition, to name a few parameters that can be macroscopically tuned. The sorting versus radius for the artificial mixture is plotted in Fig. 2a and clearly shows a high affinity of FBAR for thin tubes. Also, partitioning of the proteins for the tube was strongly dependent on the bulk concentration of FBAR. For 50 nM FBAR we measured up to 10–15 fold higher density on the tubes whereas for 500 nM FBAR the sorting was severely attenuated to approximately 2–3. This sorting behavior was measured for both the synthetic mixture in Fig. 2a as well as for the more natural composition of the brain lipid system, Fig. 2b. Similar density dependent sorting was observed for NBAR proteins on the same kind of GUV/tube system made of similar synthetic lipid mixture as shown in Fig. 2a[11,13] and was attributed to crowding effects at high density.

It is evident from Fig. 2 that the result of changing the membrane composition is not dramatic. However, this is not trivial as the brain lipid mixture and may contain additional lipid species, such as phosphoinosotides and other negatively charged lipids that facilitate binding of the FBAR domain to the membrane. Hence, experiments can be performed even at high ionic strength on brain lipid extracts. We did observe a similar sorting profile near physiological salt concentrations using brain lipid GUVs (see Supplementary Information, Fig. S2). Our observation that syndapin 1 is able to sense high curvatures with strong affinities even at near physiological salt concentrations (100 mM) suggests that curvature sensing is indeed a very pronounced and fundamental property of this protein.

Notably, in experiments with high protein concentration (500 nM) in bulk but with lipid mixtures that have lower charge density, and hence a very low affinity of FBAR for the GUV membrane, we observed high density on the tube relative to the GUV (see Fig. S3 and movie 1). This experiment shows that even at high solution concentrations the sorting efficiency can be high as long as the density on the membrane is kept low to avoid effects of crowding.

As a control for the curvature sensing of another protein, we added fluorescently labeled streptavidin (STP) to the GUVs and subsequently formed membrane tubes from the streptavidin coated GUVs', see Fig. S4 for two examples. Strong sensing was not observed for high curvature tubes, R = 18 nm, neither for [STP] = 500 nM nor for [STP] = 10 nM. Only residual up-concentrations of 1.9 and 1.5 of streptavidin on the tubes were measured for these two concentrations.

BAR domains have been reported to oligomerize into ordered lattices on tubes[16,23]. We do not expect any such effects at the low concentration where we observe the strongest sensing, since the molecular density on the membrane is low. To assess the mobility of the membrane bound protein at an initial 500 nM solution concentration, we performed fluorescence recovery after photobleaching (FRAP) experiments on both the GUV and the tube, see Fig. S5a and b. The FBAR domains on the GUV rapidly recovered to the initial unbleached value Fig. S5b (green circles), whereas the recovery on the tube (blue diamonds) was slower and only partial within the timescale of the experiment. The protein on the membrane tube diffused to recover the bleached area with a diffusion coefficient of $D = 0.6\ \mu m^2/s$, as shown in Fig. S5c. This provides an upper limit for the mobility on the tube since we cannot exclude the possible exchange of protein with the solution phase. However, we see that the recovery proceeds from the GUV reservoir towards the trapped particle thus confirming diffusive mixing with the GUV. We therefore only expect minimal exchange with the solution phase on the timescale of the FRAP experiment. Despite the protein mobility, we still observe a mechanical effect due to the protein on the bilayer when the membrane tension is suddenly decreased as shown in Fig. S6. A decrease in aspiration pressure does not immediately increase the tube diameter. Instead, the excess area results in an increase of the tube length, and the tube bends out of the focal plane of the

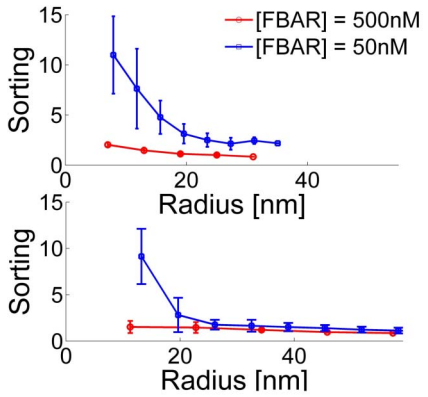

Figure 2 | FBAR sorting depends on membrane curvature and protein concentration. (a) FBAR binding to tubes made of a synthetic lipid mixture (25 mol% DOPG and 74 mol% DOPC). (b) Curvature sensing on tubes of brain lipid extracts. In both (a) and (b) the sorting is measured at protein concentrations of 50 nM (blue squares) and 500 nM (red circles). Data were collected from 17 GUVs in 11 experiments. Error bars denote the standard deviations of the data points within the bin intervals.

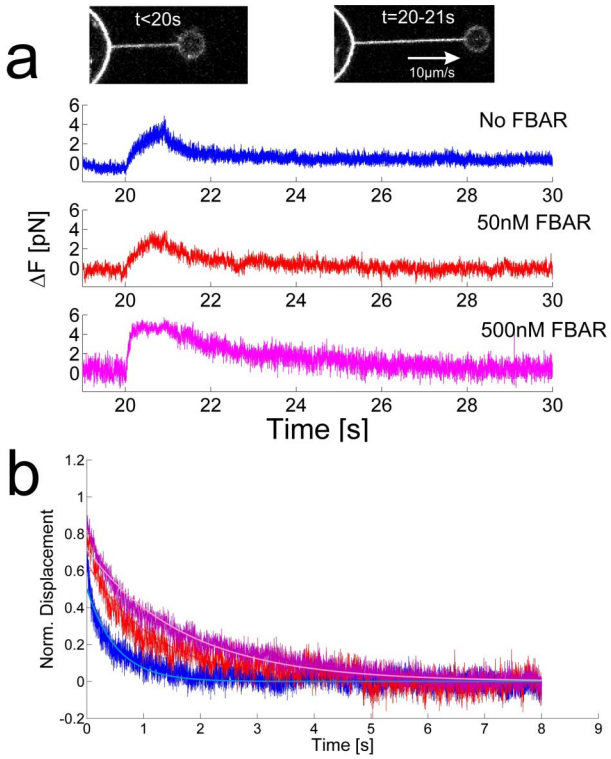

Figure 3 | Relaxation kinetics of tube restoring force after a 10 μm step elongation in the presence or absence of FBAR. The elongation is performed at 10 μm/s and the position of the particle is recorded with 45 μs time resolution. (a) Force versus time relaxation behavior of the force ΔF shown for three different concentrations of FBAR. Prior to elongation of the tether the force, F, equals the equilibrium holding force, F_h, of the short tether and $\Delta F = F - F_h = 0$. After elongation ΔF at different protein concentrations relaxes back to zero. Inset, images of GUV and tube before and after elongation (images are contrast enhanced for visibility). (b) Superimposed average relaxation behavior of a number of experiments. Experiments are performed at 500 nM (magenta, average of 8 experiments), 50 nM (red curve, average of 6 experiments) and in absence of FBAR (blue curve, average of 8 experiments). The exponential relaxation time, τ, increases with FBAR concentration with $\tau_{0\ nM} = 0.52 \pm 0.01$ s, $\tau_{50\ nM} = 1.20 \pm 0.02$ s, $\tau_{500\ nM} = 1.71 \pm 0.01$ s.

microscope (Fig. S6). This strongly implies that the protein influences the curvature elasticity of the bilayer.

Membrane relaxation depends on protein concentration. The mechanical effect of syndapin 1 on the membrane was investigated by performing a fast elongation of the tube while subsequently measuring the relaxation behavior of the force to equilibrium, see Fig. 3a. The bulk protein concentration in these experiments was held constant at 0 nM, 50 nM or 500 nM and we quantified the stabilizing effect of the protein through the decay constant of the force relaxation.

To assess the fast relaxation kinetics of elongated tethers in the presence or absence of FBAR, we measured the force, F, exerted by the optical trap during and after the rapid tether elongation, as shown in Fig. 3. The position of the particle and the force, F, was continuously monitored at 22 kHz using a photodiode detection scheme[24,25]. The optical trap was calibrated to find the spring constant κ by characterizing the harmonic trapping potential, using power spectral analysis of the particle's Brownian motion in the trap[26], see Fig. S7. The force, F, was then obtained as the displacement of the trapped particle from the trap center, Δx, times the trapping constant κ, $F = \kappa\Delta x$. The particle was brought into contact with the GUV, a short tube of 5 μm was pulled slowly, and subsequently the tube length was then rapidly extended by 10 μm at a velocity of 10 μm/s.

Figures 3a and 3b summarize the results of the force kinetics experiments. The effect of FBAR on tube relaxation kinetics can be quantified as the relaxation rates of the decaying force or displacement which are $\tau_{0\ nM} = 0.52 \pm 0.01$ s, $\tau_{50\ nM} = 1.20 \pm 0.02$ s, and $\tau_{500\ nM} = 1.71 \pm 0.01$ s respectively, see Fig. 3b. The relaxation of the force in the absence of FBAR occurs within hundreds of milliseconds, consistent with relaxation dynamics in lipid bilayers[27,28]. In the presence of FBAR, the relaxation time increases in a concentration dependent manner. The increased relaxation, which can be observed at a concentration of 50 nM (see Fig. 3) may reflect reorganization of the protein on the tube which occurs slower at higher concentrations when the proteins are in a crowded environment. The increased relaxation times at concentrations as low as 50 nM shows that FBAR from syndapin 1 has a mechanical effect on tubes at concentrations well below 8 μM at which tubulating activity of the protein was observed[16].

Syndapin 1 stiffens tubes at high density. At higher FBAR concentrations one might expect to see an increased rigidity of the tube caused by the onset of intermolecular contacts between adjacent FBAR dimers along the tube surface as supported by previous findings of FBAR lattice formation using electron microscopy[16]. Oligomerization of BAR domains on tubes can influence the rigidity of tubes by forming a lattice like structure on the tube surface. The laterally contiguous protein shell can significantly stiffen the tube in the case of strong intermolecular contacts as observed on NBAR and FBP17 FBAR domains[17].

Based on crystallography, it has been suggested that FBAR from syndapin 1 forms rather weak intermolecular interactions on tubes formed in presence of high concentrations of syndapin 1[16]. We tested this by comparing the persistence lengths of tubes containing syndapin 1 with lipid tubes containing no protein. Tubes composed of 25 mol% DOPG and 73 mol% POPC and 2 mol% TR-DHPE were formed by incubation of high concentrations of syndapin 1 with GUVs. Tubes containing no protein were simply formed by gentle hydration of a lipid film that is normally used to form GUVs, but also spontaneously forms tubes[29,30]. To keep the tubes within the focal plane of the microscope, the tube assay was conducted inside a quasi-two dimensional chamber with a height of ca. 2–5 μm that was deduced from laser reflection at the water/glass interfaces[31].

The persistence length, L_p, of lipid tubes is a function of the membrane bending rigidity, κ, and tube radius, R[32],

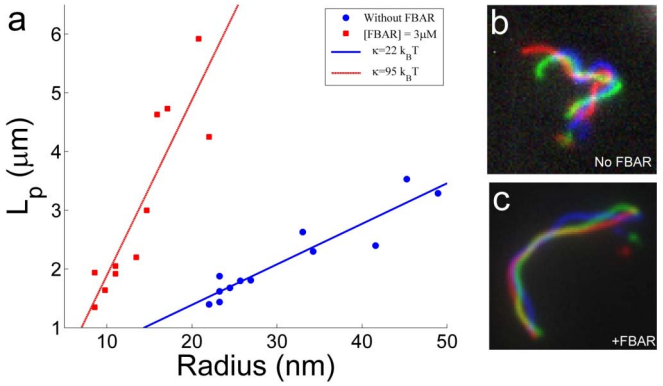

Figure 4 | Membrane tubes decorated with FBAR are stiffer than tubes without FBAR. (a) The persistence length for tubes formed at high concentrations of FBAR (red squares, 11 tubes) and bare tubes (blue circles, 12 tubes) formed by gentle hydration. (b + c) Examples of tubes having similar sizes but different stiffness as a result of binding by FBAR. The colors represent different time points separated by 884 ms. (b) No FBAR, R = 24 nm and L_p = 1.7 μm. (c) Incubated with 3 μM FBAR, R = 22 nm and L_p = 4.3 μm. The images are 13 μm × 13 μm.

$$L_p = \frac{\pi R \kappa}{k_B T}, \tag{2}$$

where $\kappa = 24\ k_BT$ is the bending rigidity for POPC membranes[33]. We used this expression to calibrate the tube radius. Unilamellarity of tubes can be assumed when tubes are formed by adding syndapin 1 to GUVs since these tubes are formed from mostly unilamellar vesicle, therefore, the intensity scales linearly with the tube radius. Tubes formed spontaneously by gentle hydration can be multilamellar which would add uncertainty to the size determination. According to eq. 2, unilamellar tubes having a persistence length of ~1–2 μm would have radii of ~20–30 nm, see blue line in Fig. 4a. If these tubes were multilamellar it would imply that the tubes were even thinner since otherwise the persistence lengths would be larger than ~1–2 μm. We consider it unlikely that tubes formed spontaneously would both have radii below 20 nm and be multlilamellar due to the high energy of bending of multilayered membranes. We measured the persistence lengths of several tubes having similar intensity, and hence similar thicknesses, thus providing an estimate of the radius, R, of the tube. Since the intensity scales linearly with radius, we could infer the radius for any tube by measuring the intensity of the membrane dye.

Consistent with the theoretical prediction of eq. 2, we measured a linear dependence of L_p on R for POPC-DOPG membrane tubes, as shown in Fig. 4 (blue circles). Using linear regression we obtained a bending rigidity of the membrane of $\kappa = 22\ k_BT$ that is consistent with the value of $\kappa = 24\ k_BT$ as measured for POPC membranes[33].

The red squares in Fig. 4 denote the persistence length of FBAR tubes of various diameters. By linear fitting of eq. 2 to the data, we find that the bending rigidity of the tubular surface has increased by nearly five fold to $\kappa = 95\ k_BT$. Hence tubes formed in presence of syndapin 1 are clearly stiffer than bare lipid tubes. The effect of FBAR on tube stiffness is illustrated in Fig. 4b and Fig. 4c in which two tubes having similar sizes are plotted at three different time points represented by three different colors. The tube in Fig. 4b contains no syndapin 1 and shows strong deflections. The tube in Fig. 4c, formed in presence of 3 μM syndapin1, however, appears much more straight.

Discussion

Knowledge about the mechanical effect and curvature sensing ability of pacsin 1/syndapin 1 is limited. Previous work has shown that

syndapin 1, unlike other proteins containing NBAR or other types of FBAR domain, does not form tubes having specific diameters that correlate with the intrinsic BAR domain curvature[16,20]. A remarkable feature of syndapin 1 is its ability to generate a range of curvatures going well above its own intrinsic concave curvature. In cells, syndapin 1 has been associated with narrow tubes at late stages of endocytosis through its interactions with mechanoenzymes such as dynamin which is known to bind to full length syndapin and relieve it from its SH3-clamped configuration[20].

We show here that the sensing of membrane curvature by syndapin 1 persists for curvatures above its intrinsic radius of curvature (~21 nm[34]) of its concave face, see Fig. 2 and Fig. S8. The sorting efficiency of FBAR continues to increase with curvature down to a tube diameter of 10–15 nm (Fig. 2). Previous work has revealed that FBAR of syndapin 1 exhibits a pronounced two dimensional curvature, allowing the domain to adopt various configurations on tubes depending on the tube radius[16]. Syndapin 1 exhibits a lateral curvature with the tip regions bent away from the central body by as much as 61°[16], which could explain its affinity for a range of curvatures including curvatures higher than the curvature of the concave face of the BAR, see Fig. S8. Moreover, syndapin 1 contains two wedge loops that are essential for the tubulating activity of the protein and could influence its sensing ability by the favored insertion of the hydrophobic loops into highly curved membranes. Sensing of another less curved FBAR (FCHo2) was reported to be enriched on small lipid vesicles, with radii down to 50 nm, by a factor of ~30. This effect was attributed to sensing by the hydrophobic part and not to the shape of the BAR domain[7]. The wedge loops on syndapin 1 are located near the distal ends of the, almost straight, central part of the protein (see Fig. S8a)[16]. Binding at an oblique angle would increase the alignment between the central part of the protein with the axis of the tube. This would lead to greater proximity between the membrane and the wedge loops, and therefore more efficient insertion of the loops into the membrane. The enrichment we measured on tubes reached 10–15 times the density on the GUV and occurred at radii down to 10–15 nm, see Fig. 2. Tubular systems pulled out of GUVs differ from lipid vesicles by having two different principal curvatures, a nonzero curvature along the azimuthal direction, and zero curvature along the tube, whereas the principal curvature of lipid vesicles are equal which could affect the curvature sensing of proteins. Also, tubes extracted from GUVs are in diffusive contact with a zero curvature membrane reservoir (GUV) thus allowing the proteins to redistribute between regions having different membrane curvature thus mimicking the membrane structures observed in endocytosis and the golgi network.

Similar results for curvature sensing, as observed here, have been obtained with NBAR domains from amphiphysin by using a similar tube/GUV assay[11,13,14]. The binding of NBAR was strongly curvature dependent at low protein concentrations and was strongly attenuated at higher densities. In ref.11 the highest sorting ratio exceeded 80 at low protein density and equaled approximately 15 at higher densities. We observed a similar strong density dependence of the sorting behavior in Fig. 2a,b where the protein concentration in solution was changed by a factor of 10. NBARs are highly curved domains with a radius of curvature of ca. 11 nm and contain N-terminal α-helices that insert into bilayers; these are two factors that could make NBAR a more efficient curvature sensor of highly curved membranes compared to the FBAR domain of syndapin 1.

Mechanical effects imposed by BAR proteins on membrane tubes have been shown for NBARs and other FBAR domain proteins[11,17]. Notably, tubes formed by the FBAR FBP17 were measured to have a persistence length of 142 μm, much stiffer than the helical coat formed by dynamin which has $L_p = 37$ μm[17]. NBARs were measured to have much shorter persistence lengths of ca. 10 μm[17]. However, despite the importance of the tube diameter in these measurements, no correlation with tube diameter was given in the above references. We measured a persistence length ranging from ca. 1.5 μm to 6 μm for tube radii between 10 nm and 25 nm, see Fig. 4a. Comparing the measured persistence lengths, in presence of FBAR, with persistence lengths of tubes in absence of FBAR we get a 5-fold increase in the tube stiffness which we attribute to the protein coat constituted by syndapin 1. This relatively weak stiffening by syndapin FBAR when compared to other FBARs and NBAR reported in Ref. 17 indicates that FBARs from syndapin 1 adopt a more labile higher order molecular arrangements on tubes as suggested in Ref. 16.

The mechanical effect of syndapin 1 was also quantified at lower concentrations (50 nM and 500 nM) by performing step elongation experiments and by measuring the kinetic force response in the holding force, as shown in Fig. 3. We observed an increase in relaxation time in presence of FBAR when compared to protein free tubes reflecting a change in the elastic response of the GUV/tube system. It is evident from Fig. 3 that the proteins act to stabilize the tube and make it less elastic. This mechanical effect is even present at 50 nM FBAR (Fig. 3, red curves). The dynamic increase in the membrane tension caused by rapid elongation relaxes within hundreds of milliseconds (see Fig. 3a), whereas the relaxation in the presence of protein is significantly slower, as seen in Fig. 3b,c. This slow down of relaxation with increasing concentrations of protein shows that crowding effects could restrict reorganization of the protein on the tube. The time dependent change in the holding force reflects the effect of the protein on the bending energy, κ, of the bilayer as can be seen from eq. S3 and eq. S4 in Supplementary Information. The stiffening of the tubes measured in Fig. 4 on the other hand reflects lateral stiffening of the tube due to the dense coat of protein on the tube surface and could originate from weak lateral interactions between the FBAR domains as reported in[16]. The time dependent change in the tube restoring force after step elongation is similar to what has been observed for other curvature generating proteins like amphiphysin NBAR[14], but is in striking contrast to the behavior observed for dynamin which showed an abrupt force change only after forming a continuous scaffolding shell around the lipid tubule extending from the GUV to the trapped particle[9].

FBARs of syndapin 1 were found to sense membrane curvatures higher than its own intrinsic curvature both on tubes formed from synthetic lipid mixtures and on tubes formed from brain lipid extracts. Up-concentration of FBAR on the tube relative to the GUV was strongly density dependent with partitioning between low and high curvatures being amplified at lower FBAR densities. Moreover, syndapin 1 was shown to mechanically perturb the membrane tube in a concentration dependent manner, as was measured by force relaxation measurements where the force decay was measured during a step elongation of the tether. Finally, by analyzing the thermal fluctuations of free tubes suspended in a 2D chamber, we measure a five-fold increase in the persistence length of tubes containing FBAR, implying that FBAR has the ability to form lateral intermolecular contacts along tubular structures that stiffen membrane tubes.

Methods

A syndapin 1 SH3 mutant Q396R/E397R, labeled with GFP, was kindly donated by Volker Hauke (Laboratory for Membrane Biochemistry & Molecular Cell Biology, Freie Universität Berlin) and stored in a salt buffer (20 mM HEPES, 150 mM NaCl, pH 7.4). Details about the mutant and the purification process are given in Ref. 20. Details of the materials used are given in Supplementary Information.

Giant unilamellar vesicles (GUVs). GUVs were prepared by electroformation using indium titanium coated slides on which the film was spread and subsequently hydrated. See Supplementary information for more details on the procedure for GUV formation and on formation of tubes.

The experimental Setup is described in Supplementary Information and the principle behind the optical trapping and calibration system is given in[24,26,35].

Step elongation experiments. A program was written in Labview (National Instruments) to control the piezo stage to perform a sequence of controlled

movements at different velocities while acquiring data from the photodiode. Initially, the stage was moved at 1 μm/s to form a tether of 5 μm, subsequently we performed two rapid pulls separated by 40 s. Each pull was performed at 10 μm/s. During the whole experiment the position of the particle was recorded by the quadrant photodiode at a 45 μs time resolution.

Data analysis. All image analysis was performed in Matlab (The MathWorks, Natick, MA). Vesicle fluorescence intensities for each channel were calculated by thresholding the images using the background level plus one standard deviation of the noise as the threshold. The integrated intensity of all pixels falling above the threshold for the GUV and the tube, respectively, were quantified for both the protein and membrane channel and the relevant ratios were quantified as described in the paper. A polarization correction factor (PCF)[22] was found by measuring the residual *Sorting* at tube diameters of R ~ 100 nm (where membrane curvature effects should be negligible) and was used to normalize the *Sorting* in all experiments. Tube persistence lengths were analyzed by a custom made Matlab program using the method described in Ref. 36.

Sample preparation. The experimental chamber for tube pulling is described in Supplementary Information. To measure the shape of freely floating tubes we made quasi-2D chambers with a height of ca. 3–5 μm as measured by laser reflection at the glass water interfaces. After coating two clean glass surfaces with α-casein we added 1 μL of solution, containing tubes, onto one glass and subsequently placed the other glass on top without any spacer. The spreading of the droplet forms a hydration layer on the glass and is sufficient for creating a thin 2D layer of a few micrometers.

Further details of the materials and methods for preparing micropipettes and the sample chamber are given in Supplemental information.

1. Dharmalingam, E. *et al.* F-BAR proteins of the syndapin family shape the plasma membrane and are crucial for neuromorphogenesis. *J Neurosci* **29**, 13315–13327 (2009).
2. McMahon, H. T. & Gallop, J. L. Membrane curvature and mechanisms of dynamic cell membrane remodelling. *Nature* **438**, 590–596 (2005).
3. Rao, Y. & Haucke, V. Membrane shaping by the Bin/amphiphysin/Rvs (BAR) domain protein superfamily. *Cell Mol Life Sci* **68**, 3983–3993 (2011).
4. Chen, Y., Aardema, J., Misra, A. & Corey, S. J. BAR proteins in cancer and blood disorders. *Int J Biochem Mol Biol* **3**, 198–208 (2012).
5. Antonny, B. Mechanisms of membrane curvature sensing. *Annu Rev Biochem* **80**, 101–123 (2011).
6. Baumgart, T., Capraro, B. R., Zhu, C. & Das, S. L. Thermodynamics and mechanics of membrane curvature generation and sensing by proteins and lipids. *Annu Rev Phys Chem* **62**, 483–506 (2011).
7. Bhatia, V. K. *et al.* Amphipathic motifs in BAR domains are essential for membrane curvature sensing. *EMBO J* **28**, 3303–3314 (2009).
8. Peter, B. J. *et al.* BAR domains as sensors of membrane curvature: the amphiphysin BAR structure. *Science* **303**, 495–499 (2004).
9. Roux, A. *et al.* Membrane curvature controls dynamin polymerization. *Proc Natl Acad Sci U S A* **107**, 4141–4146 (2010).
10. Singh, P., Mahata, P., Baumgart, T. & Das, S. L. Curvature sorting of proteins on a cylindrical lipid membrane tether connected to a reservoir. *Phys Rev E Stat Nonlin Soft Matter Phys* **85**, 051906 (2012).
11. Sorre, B. *et al.* Nature of curvature coupling of amphiphysin with membranes depends on its bound density. *Proc Natl Acad Sci U S A* **109**, 173–178 (2012).
12. Tian, A. & Baumgart, T. Sorting of lipids and proteins in membrane curvature gradients. *Biophys J* **96**, 2676–2688 (2009).
13. Zhu, C., Das, S. L. & Baumgart, T. Nonlinear sorting, curvature generation, and crowding of endophilin N-BAR on tubular membranes. *Biophys J* **102**, 1837–1845 (2012).
14. Heinrich, M. C. *et al.* Quantifying Membrane Curvature Generation of Drosophila Amphiphysin N-BAR Domains. *J Phys Chem Lett* **1**, 3401–3406 (2010).
15. Qualmann, B., Roos, J., DiGregorio, P. J. & Kelly, R. B. Syndapin I, a synaptic dynamin-binding protein that associates with the neural Wiskott-Aldrich syndrome protein. *Mol Biol Cell* **10**, 501–513 (1999).
16. Wang, Q. *et al.* Molecular mechanism of membrane constriction and tubulation mediated by the F-BAR protein Pacsin/Syndapin. *Proc Natl Acad Sci U S A* **106**, 12700–12705 (2009).
17. Frost, A. *et al.* Structural basis of membrane invagination by F-BAR domains. *Cell* **132**, 807–817 (2008).
18. Bai, X., Meng, G., Luo, M. & Zheng, X. Rigidity of wedge loop in PACSIN 3 protein is a key factor in dictating diameters of tubules. *J Biol Chem* **287**, 22387–22396 (2012).
19. Henne, W. M. *et al.* Structure and analysis of FCHo2 F-BAR domain: a dimerizing and membrane recruitment module that effects membrane curvature. *Structure* **15**, 839–852 (2007).
20. Rao, Y. *et al.* Molecular basis for SH3 domain regulation of F-BAR-mediated membrane deformation. *Proc Natl Acad Sci U S A* **107**, 8213–8218 (2010).
21. Hochmuth, R. M. & Evans, E. A. Extensional flow of erythrocyte membrane from cell body to elastic tether. I. Analysis. *Biophys J* **39**, 71–81 (1982).
22. Sorre, B. *et al.* Curvature-driven lipid sorting needs proximity to a demixing point and is aided by proteins. *Proc Natl Acad Sci U S A* **106**, 5622–5626 (2009).
23. Kessels, M. M. & Qualmann, B. Syndapin oligomers interconnect the machineries for endocytic vesicle formation and actin polymerization. *J Biol Chem* **281**, 13285–13299 (2006).
24. Hansen, P. M., Bhatia, V. K., Harrit, N. & Oddershede, L. Expanding the optical trapping range of gold nanoparticles. *Nano Lett* **5**, 1937–1942 (2005).
25. Bendix, P. M. & Oddershede, L. B. Expanding the optical trapping range of lipid vesicles to the nanoscale. *Nano Lett* **11**, 5431–5437 (2011).
26. Hansen, P. M., Tolic-Nørrelykke, I. M., Flyvbjerg, H. & Berg-Sørensen, K. Tweezercalib 2.1: Faster version of MatLab package for precise calibration of optical tweezers. *Comp Phys Comm* **175**, 572–573 (2006).
27. Zhou, H., Gabilondo, B. B., Losert, W. & van de Water, W. Stretching and relaxation of vesicles. *Phys Rev E Stat Nonlin Soft Matter Phys* **83**, 011905 (2011).
28. van Osdol, W. W., Johnson, M. L., Ye, Q. & Biltonen, R. L. Relaxation dynamics of the gel to liquid-crystalline transition of phosphatidylcholine bilayers. Effects of chainlength and vesicle size. *Biophys J* **59**, 775–785 (1991).
29. Angelova, M. I. & Dimitrov, D. S. Liposome Electroformation. *Faraday Discuss Chem Soc* **81**, 303–311 (1986).
30. Akashi, K., Miyata, H., Itoh, H. & Kinosita, K., Jr. Preparation of giant liposomes in physiological conditions and their characterization under an optical microscope. *Biophys J* **71**, 3242–3250 (1996).
31. Reihani, S. N. S., Mir, S. A., Richardson, A. C. & Oddershede, L. B.. Significant improvement of optical traps by tuning standard water immersion objectives. *J. Opt.* **13**, 1–6 (2011).
32. Derenyi, I., Julicher, F. & Prost, J. Formation and interaction of membrane tubes. *Phys Rev Lett* **88**, 238101 (2002).
33. Bouvrais, H. *et al.* Softening of POPC membranes by magainin. *Biophys Chem* **137**, 7–12 (2008).
34. Edeling, M. A. *et al.* Structural requirements for PACSIN/Syndapin operation during zebrafish embryonic notochord development. *PLoS One* **4**, e8150 (2009).
35. Richardson, A. C., Reihani, N. & Oddershede, L. B. Combining confocal microscopy with precise force-measuring optical tweezers. *SPIE Proc* **6326**, 28–38 (2006).
36. Ott, A., Magnasco, M., Simon, A. & Libchaber, A. Measurement of the persistence length of polymerized actin using fluorescence microscopy. *Phys Rev E* **48**, R1642–R1645 (1993).

Acknowledgements

The work was funded by the Danish-American Fulbright Commission (Grantee ID 34111300), The Carlsberg Foundation, the Villum Foundation, and a University of Copenhagen Center of Excellence: MolPhysX. We thank Volker Hauke (Laboratory for Membrane Biochemistry & Molecular Cell Biology, Freie Universität Berlin) for providing us with F-BAR constructs.

Author contributions

L.B.O. and P.M.B. designed the research. P.R., Y.F.B., S.N.S.R. and P.M.B. carried out experiments. P.R., L.B.O. and P.M.B. wrote the main manuscript text. P.R. and P.M.B. analyzed the sorting data. Y.F.B. measured and analyzed the tube persistence lengths. S.N.S.R. wrote labview software for kinetic pulling experiments. D.S. contributed with reagents. All authors reviewed the manuscript.

Additional information

Supplementary information accompanies this paper at http://www.nature.com/scientificreports

Competing financial interests: The authors declare no competing financial interests.

How to cite this article: Ramesh, P. *et al.* FBAR Syndapin 1 recognizes and stabilizes highly curved tubular membranes in a concentration dependent manner. *Sci. Rep.* **3**, 1565; DOI:10.1038/srep01565 (2013).